Loss of synchronization in complex neuronal networks with delay

Judith Lehnert[1], Thomas Dahms[1], Philipp Hövel[1,2] and Eckehard Schöll[1] (a)

[1] *Institut für Theoretische Physik, Technische Universität Berlin, Hardenbergstraße 36, 10623 Berlin, Germany*
[2] *Bernstein Center for Computational Neuroscience Berlin, Philippstraße 13, Haus 2, 10115 Berlin, Germany*

PACS 05.45.Xt – Synchronization, nonlinear dynamics
PACS 87.85.dq – Neural network
PACS 89.75.-k – Complex system

Abstract – We investigate the stability of synchronization in networks of delay-coupled excitable neural oscillators. On the basis of the master stability function formalism, we demonstrate that synchronization is always stable for excitatory coupling independently of the delay and coupling strength. Superimposing inhibitory links randomly on top of a regular ring of excitatory coupling, which yields a small-world-like network topology, we find a phase transition to desynchronization as the probability of inhibitory links exceeds a critical value. We explore the scaling of the critical value in dependence on network properties. Compared to random networks, we find that small-world topologies are more susceptible to desynchronization via inhibition.

Introduction. – Studies of complex networks have sparked tremendous scientific activities in many research areas and the analysis of network topologies in real-world systems has become a field of large interest. For instance, there is evidence that neuronal networks on the level of single neurons coupled through synapses or gap junctions, as well as on the level of cortex areas and their pathways exhibit the small-world (SW) properties [1,2]. The high clustering coefficient of the SW networks enhances local communication efficiency, while the small shortest path length enables efficient global communication [3]. Thus, the SW architecture is optimal for processing and transmission of signals within and between brain areas. However, the synchronizability of small-world networks depends in a delicate way upon the network topology [4]. Next to this structural aspect, inhibition plays a prominent role in many neural processes [5]. Without an inhibitory mechanism, excitation in a compound system would not decay, but spread through the whole network, finally leading to persistent spiking of all neurons. Thus, encoding and processing of information would be impossible.

In this Letter, we combine both fundamental aspects – inhibition and SW property – in order to emphasize the important interplay of excitation and inhibition in complex networks. We start with a regular ring network that consists of purely excitatory links with delay. Thus, it exhibits strong and stable synchronization. Depending on the initial conditions, both isochronous and cluster synchronization are possible implying multistability. Additional inhibitory connections, which we include in a SW-like manner [1, 6], result in a loss of synchronization. A similar transition was reported for phase oscillators in Ref. [7] for unidirectional rings, but the effect of inhibition upon excitable systems could not be treated by that model. For the node dynamics, we consider a generic model to demonstrate the fundamental relevance and importance of our findings in the field of neuroscience. In this area, synchronization can be related to cognitive capacities [8] as well as to pathological conditions, e.g., epilepsy [9]. A better understanding of the loss of synchronization will eventually lead to future therapeutic treatments [10].

Throughout this Letter, we consider a network of N delay-coupled FitzHugh-Nagumo (FHN) oscillators. The FHN system describes neuronal dynamics by a two-variable model [11]. Because of its simplicity it can be considered as a paradigmatic model of excitable systems, which also occur in several other natural contexts ranging from cardiovascular tissues to the climate system [12, 13].

(a) E-mail: schoell@physik.tu-berlin.de

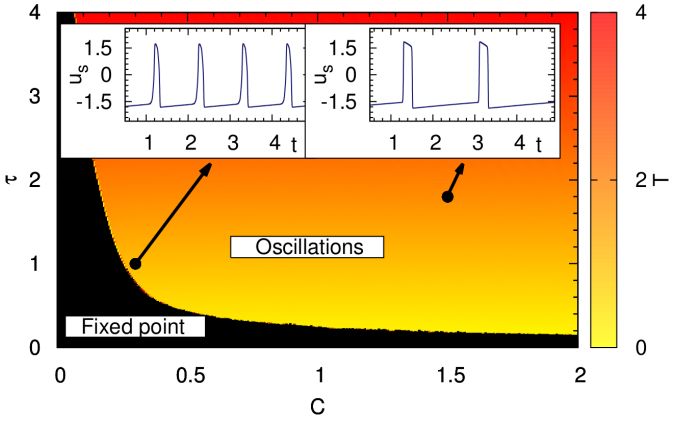

Fig. 1: (Color online) Dynamics in the synchronization manifold in dependence on the coupling strength C and delay τ. The gray scale (color code) indicates the period of spiking oscillations T, the black region corresponds to fixed-point dynamics. Left and right insets show time series of the activator u_s for ($C = 0.3$, $\tau = 1$) and ($C = 1.5$, $\tau = 1.8$), respectively. Parameters: $a = 1.3$, $\epsilon = 0.01$.

Here, the network dynamics is described by

$$\epsilon \dot{u}_i = u_i - \frac{u_i^3}{3} - v_i + C \sum_{j=1}^{N} G_{ij}[u_j(t-\tau) - u_i] \quad (1a)$$

$$\dot{v}_i = u_i + a, \quad (1b)$$

where u_i and v_i denote the activator and inhibitor variables of the nodes $i = 1, \ldots, N$, respectively. The parameter a determines the threshold of excitability. A single FHN oscillator is excitable for $a > 1$ and exhibits self-sustained periodic firing beyond the Hopf bifurcation at $a = 1$. Here, we will focus on the excitable regime with $a = 1.3$. The time-scale parameter ϵ is chosen as $\epsilon = 0.01$. C is the coupling strength. $\mathbf{G} = \{G_{ij}\}$, $i, j = 1, \ldots, N$, denotes the coupling matrix that determines the topology of the network. In the following we will assume unity row sum of $\mathbf{G}$. This ensures that each neuron receives the same input if the network is synchronized. The delay time τ takes into account the finite propagation speed of an action potential. We investigate complete synchronization with $(u_i(t), v_i(t)) = (u_s(t), v_s(t)) \equiv \mathbf{x}_s(t)$ for $i = 1, \ldots, N$, which is also known as zero-lag or isochronous synchronization. This state is a solution of qs. (1) and reduces the system's dynamics to

$$\dot{\mathbf{x}}_s = \mathbf{F}(\mathbf{x}_s) + C\mathbf{H}\left[\mathbf{x}_s(t-\tau) - \mathbf{x}_s(t)\right] \quad (2)$$

with $\mathbf{F}(\mathbf{x}) = \begin{pmatrix} [u - u^3/3 - v]/\epsilon \\ u + a \end{pmatrix}$ and the matrix $\mathbf{H} = \begin{pmatrix} 1/\epsilon & 0 \\ 0 & 0 \end{pmatrix}$. The $2(N-1)$ constraints of complete synchronization define a two-dimensional synchronization manifold (SM) in the $2N$-dimensional phase space.

As we operate in the excitable regime, the dynamics on this SM, in particular the period, will depend on the choice of the coupling parameters C and τ as depicted in fig. 1. The grayscale (color code) corresponds to the period T of the oscillations on the SM, which we find to follow $T = \tau + \delta$ with $\delta \ll \tau$ accounting for a short activation time [14]. For small coupling strength C the incoming signal is not sufficient to trigger oscillations (black region). For small delay times τ consecutive spikes run into the refractory phase of the previous one, which prevents oscillations as well. From here on we consider C and τ sufficiently large such that the coupling induces oscillations.

Stability analysis. – In the following we address the question whether the oscillatory solution on this manifold is transversely stable. The master stability function (MSF) [15] allows us to quantify this transversal stability. It can be calculated as largest Lyapunov exponent Λ from eq. (1) linearized around eq. (2):

$$\dot{\boldsymbol{\zeta}}(t) = [D\mathbf{F}(\mathbf{x}_s(t)) - C\mathbf{H}]\,\boldsymbol{\zeta}(t) + (\alpha + i\beta)\mathbf{H}\boldsymbol{\zeta}(t-\tau). \quad (3)$$

Here, $D\mathbf{F}$ denotes the Jacobian of $\mathbf{F}$. The idea of the MSF is to calculate the stability of a synchronized solution for an arbitrary topology matrix $\mathbf{G}$. For this purpose, the parameter $\alpha + i\beta$ represents a continuous parametrization of $\{C\nu_i\}$, where ν_i, $i = 1, \ldots, N$, are the eigenvalues of $\mathbf{G}$. In the same sense, the vector $\boldsymbol{\zeta}$ is a generalization of the variational vectors transformed to the corresponding eigensystem. In the (α,β)-plane the MSF typically gives rise to regions with negative Λ. If all rescaled transversal eigenvalues $\{C\nu_i\}$ of a given network are located within this stable region, perturbations from the SM will decay exponentially and the synchronized dynamics will be stable. Due to the unity row sum condition, $\mathbf{G}$ will always have one eigenvalue $\nu_1 = 1$. This longitudinal eigenvalue is associated with perturbations within the SM and is not relevant for the stability of synchronization. $\Lambda(C\nu_1)$ determines the type of dynamics on the SM. For periodic dynamics in the SM, as in the present case, we have $\Lambda(C\nu_1) = 0$.

Figure 2 depicts the MSF for the network of FHN oscillators given by eqs. (1). Dark (blue) colors mark the stable region. As an illustration the rescaled eigenvalues $\{C\nu_i\}$ of a bidirectionally coupled ring ($N = 8$) are shown as red symbols. The corresponding coupling matrix is given by $G_{i,i+1 \bmod N} = G_{i,i-1 \bmod N} = 1$ ($i = 1, \ldots, N$) and zero otherwise. The rescaled longitudinal eigenvalue $C\nu_1 = C$ is depicted by a black (red) square. All rescaled transversal eigenvalues (black (red) circles) lie inside the stable region indicating that the synchronization of the bidirectionally coupled ring is stable.

Shape of stability region. – The MSF must be calculated for each combination of C and τ. Although different C and τ lead to quantitatively different Lyapunov exponents Λ, the shape of the stable regions remains qualitatively very similar. In particular, it is in very good approximation given by the circle $S((0,0), C)$ with center at the origin and radius C (dotted circle in fig. 2) independent of the specific values of C and τ. The rotational symmetry has recently been proved generally for large τ [16].

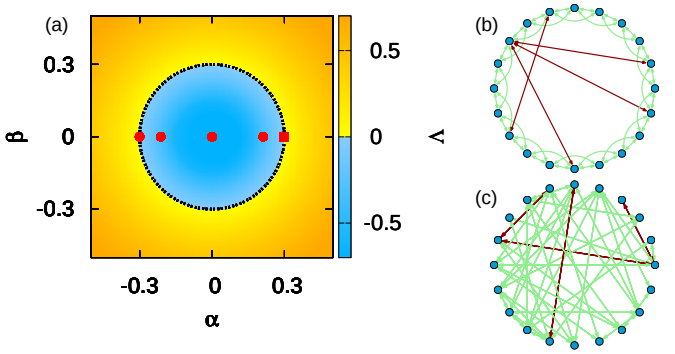

Fig. 2: (Color online) (a) Master stability function for a network of FHN systems given by eqs. (1). Dotted curve: $S((0,0),C)$. Red circles (square): Rescaled transversal (longitudinal) eigenvalues $C\nu_i$ of a bidirectionally coupled ring with $N = 8$ nodes. Parameters: $a = 1.3$, $\epsilon = 0.01$, $C = 0.3$, $\tau = 1$. (b) Scheme of a bidirectional regular network ($N = 20$, $k = 2$), and (c) a random network ($N = 20$, fixed number of links kN) with excitatory coupling (gray (green) arrows) on which inhibitory links (black (red) arrows) are superimposed.

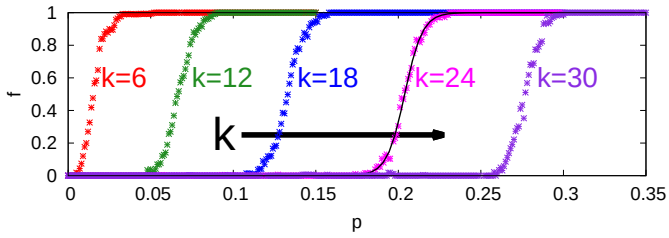

Fig. 3: (Color online) Fraction of desynchronized networks f vs the probability of additional inhibitory links p for $N = 100$. k varies from 6 to 30. Thin black curve: Example fit to $f(p)$ ($p_c = 0.20387$, $b = 186$) for $k = 24$. Number of realizations: 500 for each value of k. Parameters as in fig. 1.

Only for small τ and C the stable region is slightly larger than the circle and shows a bulge around $\alpha = -C$, $\beta = 0$ [17]. The positive α-axis is always intersected at $\alpha = C$, which corresponds to $\Lambda(C\nu_1) = 0$ as discussed above. For any choice of τ and C that leads to periodic dynamics on the SM, the circle $S((0,0),C)$ serves as a lower bound for the stability boundary. See the appendix for an analytic derivation of this circle $S((0,0),C)$ in the limit of large coupling strength and as a lower bound for all coupling strengths. We conclude that the stability of the synchronized periodic dynamics, if such a solution exists, depends only on the topology and neither on the coupling strength nor on the delay time.

Excitatory coupling. – For excitatory coupling, i.e., $G_{ij} \geq 0$, all eigenvalues of $\mathbf{G}$ are located inside the stable region. Using Gershgorin's circle theorem [18], which gives an upper bound of the eigenvalues, and the constant row sum assumption, all Gershgorin circles ($i = 1, \ldots, N$), centered at G_{ii} with radius $\sum_{j\neq i} G_{ij} = 1 - G_{ii}$ because of the unity row sum, lie inside the unit circle. Thus all rescaled eigenvalues $\{C\nu_i\}$, $i = 1, \ldots, N$, are located inside $S((0,0),C)$, i.e., inside the stable region. Networks with purely excitatory coupling will always exhibit stable synchronization.

Inhibitory coupling. – As a consequence of this result, desynchronization can only be achieved by introducing negative entries in the coupling matrix $\mathbf{G}$, i.e., inhibitory coupling between neurons. This inhibition is a crucial feature in neural processes, e.g., to overcome unwanted synchronization associated with pathological states.

Particularly, we consider the following variation of the Watts-Strogatz SW network [1, 6]: (i) Start with a one-dimensional ring of N nodes, where every node is connected by excitatory links to its k neighbors on either side. (ii) For each of the kN links of the network add an inhibitory link with probability p connecting two randomly chosen nodes. (iii) Do not allow self-coupling or more than one link between any pair of nodes. (iv) Normalize the entries of the coupling matrix $\mathbf{G}$ by dividing each row by the absolute value of its row sum. In the case that the row sum of the ith row is negative we set $G_{ii} = 2$ to ensure unity row sum. Figure 2(b) illustrates such a SW network for $N = 20$ and $k = 2$, where gray (green) and black (red) arrows indicate excitatory and inhibitory coupling, respectively. For each realization of such a network, we determine the stability of synchronization by checking whether the full eigenspectrum $C\nu_i$ of the coupling matrix is contained in the stable region $S((0,0),C)$. Hereby we compute the fraction f of desynchronized networks. Figure 3 shows f as a function of p for different coupling ranges k. This Figure is virtually identical for all delay times, that is, for all parameters within the color shaded area of Fig.1. To obtain this Figure we made use of the circular shape of the stable region of the master stability function. Only for very small delays or coupling strength, the stable region is slightly larger and thus the shape of the curves shown in Figure 3 might be shifted slightly to larger values of p.

For fixed k a steep transition between synchronization and desynchronization takes place as p approaches a critical value p_c. This critical value p_c and the steepness b of the transition can be fitted with a sigmoidal function $f(p) = 1/[e^{-b(p-p_c)} + 1]$. Figure 4(a) depicts the critical probability p_c for $f(p_c) = 0.5$ in dependence on k/N for different network sizes. It can be seen that for SW networks p_c follows a linear relation $p_c(k/N) = 1.16k/N - 0.07$ independently of the network size N. Figure 4(c) shows the steepness b as a function of the network size demonstrating that the transition becomes increasingly sharp as N increases. This indicates a first-order nonequililibrium phase transition in the thermodynamic limit [23].

To verify whether this phase transition and especially its independence of the network size is common in networks with inhibitory links or unique to the SW structure, we

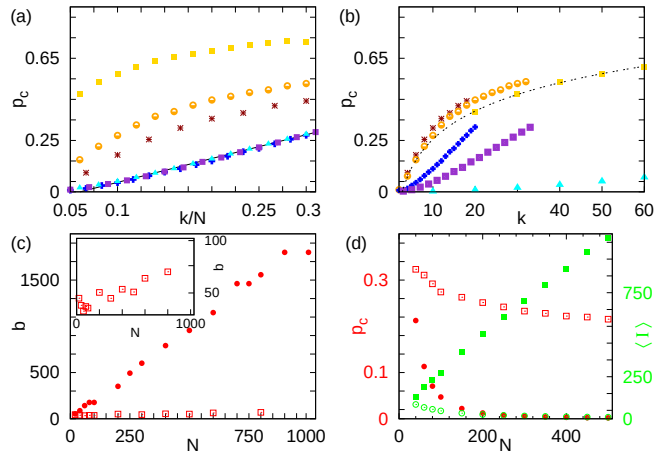

Fig. 4: (Color online) Critical value p_c for different network sizes, (a) in dependence on k/N, (b) in dependence on k: SW networks $N = 60$ (dark (blue) circles), $N = 100$ (dark (purple) squares), and $N = 500$ (turquoise triangles). Random networks $N = 60$ (black (red) crosses), $N = 100$ (light (orange) circles), and $N = 500$ (lightgray (yellow) squares). (c) Steepness b for SW (circles) and random (squares) networks vs. N for constant $k/N = 0.1$. Inset: Blow-up for random networks. (d) p_c vs. N for $k = 10$ for a SW (black (red) filled circles) and a random (black (red) empty squares) network. Number of inhibitory links $\langle I \rangle$ vs. N for constant k for a SW (gray (green) empty circles) and a random (gray (green) filled squares) network. Number of realizations: 500.

construct a different network for comparison: The regular excitatory network is replaced by a random network with fixed number of excitatory links kN equivalently to the regular network used before, as shown in fig. 2(c). We only consider realizations where this underlying excitatory network is fully connected. The construction of the inhibitory links then follows steps (ii-iv) as above. We find that a phase transition to desynchronization still occurs with critical probabilities of inhibitory links p_c as depicted in fig. 4(a) by black (red) crosses, gray (orange) circles, and lightgray (yellow) squares for $N = 60$, 100, and 500, respectively. We observe, however, that the values of p_c are higher, i.e., the random network can tolerate more inhibitory links than the SW network before desynchronizing. Furthermore, the function $p_c(k/N)$ is no longer independent of the network size N. Instead, p_c is a function of $\log(k)$ as can be seen in fig. 4(b), where p_c is plotted in dependence on k for the different network sizes N. Figure 4(d) depicts p_c in dependence on N for constant $k = 10$ for a random (black (red) empty squares) and for a SW network (red (gray) circles). For random networks, p_c is independent of N for sufficiently large N, while for SW networks it approaches zero. Recall that p_c is the mean value of the ratio of inhibitory to excitatory links. Thus, we conclude that in SW networks with increasing network size N but same local structure (constant k) an infinitesimally small ratio of inhibition to excitation is needed to prevent synchronization, while in a random network even for very large networks only a non-vanishing ratio impairs synchronization. We find in a SW network with constant k that the mean value of the number of inhibitory links $\langle I \rangle := p_c kN$ causing desynchronization scales as $\langle I \rangle = 1.16k^2 - 0.07kN$ for small N and approaches zero for large N (see fig. 4(d) green (gray) empty circles). In contrast, in a random network $\langle I \rangle$ is proportional to N (see fig. 4(d) green (gray) filled squares), i.e., an increasing number of inhibitory links is needed. This difference to SW networks can be understood in an intuitive way: In a SW, any added inhibitory link is part of a shortest path for many pairs of nodes, as it shortens the mean path length considerably with respect to the underlying regular ring. In the random network, however, where the mean path length is relatively low even without added shortcuts, only few node pairs will gain shorter paths by adding inhibitory links. Considering the dynamics on a network, perturbations from the synchronized state spread along the shortest paths first, changing the response of the receiving node, and information flow along longer paths will reach the receiving node only at a later time and will not influence the change of the initial response. In conclusion, if a large fraction of the inhibitory links is part of the shortest paths - like in the small-world topology superimposed to a regular ring - these inhibitory shortcuts become dominant.

Conclusions. – We have shown how the interplay of excitatory and inhibitory couplings leads to desynchronization in networks of neural oscillators. The desynchronization is achieved via a phase transition from a completely synchronized state. This can be seen as a first step towards an understanding of the robustness of different states of synchrony, e.g., cluster synchronization, in arbitrary networks with weighted links or distributed delays. Note that for appropriate network topologies the framework of the MSF presented above can indeed be extended to cluster synchronization where the oscillators synchronize in M clusters with a constant phase lag $2\pi/M$ between subsequent clusters [19]. The corresponding SM is $2M$ dimensional. Hence, M longitudinal eigenvalues exist. The MSF, however, is again very well approximated by the circle $S((0,0), C)$ and thus, we observe multistability between zero-lag and cluster synchronization.

Excitable systems can be classified into type-I and type-II excitability [13, 20]. In addition to the generic type-II FitzHugh-Nagumo model used in this paper, we have considered the normal form of a *saddle-node bifurcation on an invariant circle* (SNIC) as a generic model of type-I excitability [21]. For sufficiently large delay times and coupling strength the MSF is again given by the circle $S((0,0), C)$ implying that the previously obtained results persist. In particular, the same phase transition occurs. This indicates that the phenomena observed here are generic for any excitable system.

Appendix: Analytic approximation of the stability region. – The numerical calculation of the master

stability function has shown that $S((0,0),C)$ is a lower bound and a very good approximation of the stable region for all τ and C. As τ and C increase the approximation becomes even better. A Taylor expansion as done in Ref. [22] for the investigation of time-delayed feedback control of an unstable periodic orbit gives analytic insight in the problem. This analysis is very general and does not use the specific form of the local dynamics in terms of the FHN model. It only assumes that the synchronized dynamics is oscillatory with period T. Using a Floquet ansatz $\boldsymbol{\zeta} = e^{(\Lambda+i\Omega)t}\mathbf{Q}(t)$ with the periodic function $\mathbf{Q}(t) = \mathbf{Q}(t+T)$ in Eq. (3) yields

$$\begin{aligned}&(\Lambda + i\Omega)\mathbf{Q}(t) + \dot{\mathbf{Q}}(t) \qquad (4)\\ &\quad = (D\mathbf{F} - C\mathbf{H})\mathbf{Q}(t) + (\alpha + i\beta)e^{-(\Lambda+i\Omega)\tau}\mathbf{H}\mathbf{Q}(t-\tau).\end{aligned}$$

$\Lambda + i\Omega$ is the Floquet exponent, whose real part coincides with the Lyapunov exponent in the case of a periodic orbit.

Assume $T = \tau$. In the case of the FHN system this is an approximation since the period of the oscillations differs by a small activation time $\delta \ll \tau$ from the delay time τ following $T = \tau + \delta$. Then $\mathbf{Q}(t-\tau)$ can be substituted by $\mathbf{Q}(t)$:

$$\begin{aligned}&(\Lambda + i\Omega)\mathbf{Q}(t) + \dot{\mathbf{Q}}(t) \qquad (5)\\ &\quad = (D\mathbf{F})\mathbf{Q}(t) + \underbrace{[-C + (\alpha + i\beta)e^{-(\Lambda+i\Omega)\tau}]}_{\kappa}\mathbf{H}\mathbf{Q}(t).\end{aligned}$$

We expand the solution $\Gamma(\kappa) = \Lambda + i\Omega$ of the eigenvalue problem defined by Eq. (5) in a Taylor approximation:

$$\Gamma(\kappa) = \Gamma(0) + \Gamma'(0)\kappa + O(\kappa^2). \qquad (6)$$

Using $\Gamma(0) \equiv \lambda + i\omega$ and $\Gamma'(0) \equiv \chi' + i\chi''$ we obtain

$$\Lambda + i\Omega = \lambda + i\omega + (\chi' + i\chi'')[-C + (\alpha + i\beta)e^{-(\Lambda+i\Omega)\tau}]. \qquad (7)$$

Note that $\kappa = 0$ if $(\alpha,\beta) = (C,0)$ corresponding to the dynamics within the synchronization manifold. Thus the first term in the Taylor approximation corresponds to the Goldstone mode, i.e., $\lambda + i\omega = 0$ for $(\alpha,\beta) = (C,0)$. Equation (7) then becomes

$$\Lambda + i\Omega = \chi'[-C + (\alpha + i\beta)e^{-(\Lambda+i\Omega)\tau}]. \qquad (8)$$

Here, we assume $\chi'' = 0$. Separating Eq. (8) into real and imaginary part leaves us with

$$\begin{aligned}\Lambda &= \chi'\{-C + e^{-\Lambda\tau}[\alpha\cos(\Omega\tau) + \beta\sin(\Omega\tau)]\},\\ \Omega &= \chi' e^{-\Lambda\tau}[-\alpha\sin(\Omega\tau) + \beta\cos(\Omega\tau)]. \qquad (9)\end{aligned}$$

Equation (9) can be solved numerically yielding the circular stability region. On the border of the stability the real part of the Floquet exponent vanishes. Using $\Lambda = 0$ in Eq. (9) yields after algebraic manipulations:

$$\begin{aligned}\alpha_b &= \frac{-\Omega\sin(\Omega\tau)}{\chi'} + C\cos(\Omega\tau),\\ \beta_b &= \frac{\Omega\cos(\Omega\tau)}{\chi'} + C\sin(\Omega\tau), \qquad (10)\end{aligned}$$

where α_b and β_b denote the values of α and β, respectively, on the bounder of stability. Finally we obtain

$$\alpha_b^2 + \beta_b^2 = C^2 + \frac{\Omega^2}{\chi'^2}. \qquad (11)$$

Obviously $\alpha_b^2 + \beta_b^2 > C^2$ holds, demonstrating that $S((0,0),C)$ is a lower bound for the stable region. For large C the term C^2 on the right hand side dominates. Thus, the boundary of stability is very well approximated by $S((0,0),C)$ for large coupling strength.

* * *

This work was supported by DFG in the framework of SFB 910. PH acknowledges support by the BMBF under the grant no. 01GQ1001B (*Förderkennzeichen*).

REFERENCES

[1] D. J. Watts and S. H. Strogatz, Nature **393**, 440 (1998).
[2] O. Sporns, G. Tononi, and G. M. Edelman, Cereb. Cortex **10**, 127 (2000); O. Shefi *et al.*, Phys. Rev. E **66**, 021905 (2002); O. Sporns, Biosystems **85**, 55 (2006); C. J. Honey *et al.*, Proc. Natl. Acad. Sci. U.S.A. **104**, 10240 (2007); O. Sporns, C. J. Honey, and R. Kötter, PLoS ONE **2**, e1049 (2007).
[3] V. Latora and M. Marchiori, Phys. Rev. Lett. **87**, 198701 (2001).
[4] T. Nishikawa *et al.*, Phys. Rev. Lett. **91**, 014101 (2003).
[5] B. Haider *et al.*, J. Neurosci. **26**, 4535 (2006).
[6] R. Monasson, Eur. Phys. J. B **12**, 555 (1999); M. E. J. Newman and D. J. Watts, Phys. Lett. A **263**, 341 (1999).
[7] R. Tönjes, N. Masuda, and H. Kori, Chaos **20**, 033108 (2010).
IS03
[8] W. Singer, Neuron **24**, 49 (1999).
[9] P. J. Uhlhaas and W. Singer, Neuron **52**, 155 (2006).
[10] C. Hauptmann and P. A. Tass, Biosystems **89**, 173 (2007).
[11] R. FitzHugh, Biophys. J. **1**, 445 (1961); J. Nagumo, S. Arimoto, and S. Yoshizawa., Proc. IRE **50**, 2061 (1962).
[12] J. D. Murray, *Mathematical Biology*, Vol. 19 of *Biomathematics Texts*, 2nd ed. (Springer, Berlin Heidelberg, 1993); A. S. Mikhailov, *Foundations of Synergetics Vol. I*, 2 ed. (Springer, Berlin, 1994); J. P. Keener and J. Sneyd, *Mathematical physiology* (Springer, New York, Berlin, 1998); C. Koch, *Biophysics of Computation: Information Processing in Single Neurons* (Oxford University Press, New York, 1999); H. J. Wünsche *et al.*, Phys. Rev. Lett. **88**, 023901 (2001); A. Ganopolski and S. Rahmstorf, Phys. Rev. Lett. **88**, 038501 (2002).
[13] E. M. Izhikevich, Int. J. Bifurc. Chaos **10**, 1171 (2000).
[14] E. Schöll *et al.*, Phil. Trans. R. Soc. A **367**, 1079 (2009); M. A. Dahlem *et al.*, Int. J. Bifur. Chaos **19**, 745 (2009).
[15] L. M. Pecora and T. L. Carroll, Phys. Rev. Lett. **80**, 2109 (1998).
[16] V. Flunkert *et al.*, Phys. Rev. Lett. **105**, 254101 (2010).
[17] E.g., for $C = 0.3$ and $\tau = 1$ the radius is 0.303 in the direction of the negative α-axis.

[18] M. G. Earl and S. H. Strogatz, Phys. Rev. E **67**, 036204 (2003); C.-U. Choe *et al.*, Phys. Rev. E **81**, 025205(R) (2010).
[19] F. Sorrentino and E. Ott, Phys. Rev. E **76**, 056114 (2007); I. Kanter *et al.*, Europhys. Lett. **93**, 66001 (2011).
[20] A. L. Hodgkin, J. Physiol. **107**, 165 (1948).
[21] G. Hu *et al.*, Phys. Rev. Lett. **71**, 807 (1993).
[22] W. Just *et al.*, Phys. Rev. Lett. **78**, 203 (1997).
[23] E. Schöll, *Nonequilibrium Phase Transitions in Semiconductors* (Springer, Berlin, 1987).